Cellular Signalling 85 (2021) 110048

Contents lists available at ScienceDirect

Cellular Signalling

journal homepage: www.elsevier.com/locate/cellsig

Targeting integrated stress response regulates microglial M1/M2 polarization and attenuates neuroinflammation following surgical brain injury in rat

Teng-chao Huang [a,b,1], Lun Luo [a,1], Shi-hai Jiang [c,d,1], Chuan Chen [a], Hai-yong He [a], Chao-feng Liang [a], Wen-sheng Li [a], Hui Wang [a], Lei Zhu [e], Kun Wang [c,*], Ying Guo [a,*]

[a] Department of Neurosurgery, Third Affiliated Hospital of Sun Yat-sen University, Canton 510630, PR China
[b] East China Institute of Digital Medical Engineering, Shangrao 334000, PR China
[c] Department of Joint Replacement and Trauma Surgery, Third Affiliated Hospital of Sun Yat-sen University, Canton 510630, PR China
[d] Institute for Laboratory Medicine, Clinical Chemistry and Molecular Diagnostics, University Hospital Leipzig, Germany
[e] Department of Burns, Plastic & Reconstructive Surgery, Third Affiliated Hospital of Sun Yat-sen University, Canton 510630, PR China.

ARTICLE INFO

Keywords:
ISRIB
Integrated stress response
Surgical brain injury
Microglia
M1/M2
Neuroinflammation

ABSTRACT

Integrated stress response (ISR) contributes to various neuropathological processes and acting as a therapy target in CNS injuries. However, the fundamental role of ISR in regulating microglial polarization remains largely unknown. Currently no proper pharmacological approaches to reverse microglia-driven neuroinflammation in surgical brain injury (SBI) have been reported. Here we found that inhibition of the crucial ISR effector, activating transcription factor 4 (ATF4), using the RNA interference suppressed the lipopolysaccharide (LPS)-stimulated microglial M1 polarization *in vitro*. Interestingly, counteracting ISR with a small-molecule ISR inhibitor (ISRIB) resulted in a significant microglial M1 towards M2 phenotype switching after LPS treatment. The potential underlying mechanisms may related to downregulate the intracellular NADPH oxidase 4 (NOX4) expression under the neuroinflammatory microenvironment. Notably, ISRIB ameliorated the infiltration of microglia and improved the neurobehavioral outcomes in the SBI rat model. Overall, our findings suggest that targeting ISR exerts a novel anti-inflammatory effect on microglia via regulating M1/M2 phenotype and may represent a potential therapeutic target to overcome neuroinflammation following SBI.

1. Introduction

Surgical brain injury (SBI), as a surgical complication, is inevitably induced by daily neurosurgical procedures [1]. Early and delayed destruction of the blood-brain-barrier (BBB) leading to brain edema, cerebral ischemia, cell death, and long-term neuroinflammation [2–4]. Neuroinflammation is linked to dysregulated microglial activation, oxidative stress, neuron apoptosis, neurodegeneration, and cognitive impairment in brain injury [5]. Previous experimental data have shown that neuroinflammation plays a critical role in SBI physiopathology development [6,7]. Although the animal study providing therapeutic approaches has made progress [8], translated to the clinic has not yet succeeded [9]. A better understanding of the neuroinflammatory pathophysiology in SBI and subsequently identifying potential therapeutic interventions provides a promising strategy to achieve favorable outcomes for survivors.

Microglia are functioned throughout the central nervous system (CNS) to impel an innate immune response for maintaining neural homeostasis [10]. It is gradually realized that microglia are the first responders and the important mediators to SBI or traumatic brain injury (TBI) [11]. In response to brain injuries, activated microglia cells polarize toward the inflammatory M1 phenotype, resulting in increased production of proinflammatory cytokines including interleukin (IL)-1β, IL-6, and tumor necrosis factor (TNF)-α [12]. Microglial infiltration into the injury sites is necessary for subsequent brain injury restoration [4,13]. However, prolonged microglial accumulation in dysregulated resolution phase establishes a highly and continuously inflammatory neuroenvirment. In vivo study demonstrated that attenuating M1

* Corresponding authors.
E-mail addresses: wangk@mail.sysu.edu.cn (K. Wang), guoy@mail.sysu.edu.cn (Y. Guo).
[1] These authors contributed equally to this work.

https://doi.org/10.1016/j.cellsig.2021.110048
Received 7 February 2021; Received in revised form 1 May 2021; Accepted 16 May 2021
Available online 17 May 2021

microglia-mediated neuroinflammation was beneficial to the neurological outcome after SBI [14]. Moreover, reducing the M1/M2 microglial ratio has been reported to attenuate neuroinflammation [15]. Therefore, modulation of the M1/M2 phenotype of the microglia may be a novel strategy for neuroprotection and neuroinflammation resolution in SBI.

Integrated stress response (ISR), an evolutionarily conservative and central signaling network, responds to environmental stress by transforming a selected protein translation reprogramming [16]. The ISR contributes to the pathogenesis of memory deficits, cognitive disorders, and neurodegeneration accompanied by inflammation. Interestingly, systemic inhibition of ISR with the small molecule inhibitor ISRIB after TBI can reverse the long-term memory deficits [17]. Studies have investigated the role of ISR acting as a therapeutic target for CNS injuries [18]. In vitro study suggested that suppressing the ISR activating axis, mainly the eukaryotic translation initiation factor 2α (eIF2α)/activating transcription factor 4 (ATF4) signaling pathway, attenuates the M1 microglia-mediated generation of proinflammatory cytokines [19]. However, activation of the GCN2/eIF2α/ATF4 signaling pathway was also found to reduces neuroinflammation after intracerebral hemorrhage disorder [20]. A recent report demonstrated that administration of ISRIB could rescue protein synthesis in the hippocampus of Alzheimer's disease model [21]. Therefore, exploring the actual biological connection between ISR and microglial polarization is urgently needed.

In this study, we hypothesized that ISR may contribute to the regulation of M1/M2 phenotype polarization of microglia, and integrated stress response inhibitor ISRIB could counteract neuroinflammation after experimental SBI. We aimed to investigate the role of ATF4 and ISRIB in regulating phenotype transformation of activated microglia. The presented results may provide the first evidence of a possible anti-inflammatory effect on SBI-induced microglia activation by targeting ISR.

2. Materials and methods

2.1. Animals

All experiments were conducted following the National Institutes of Health (NIH) Guide for the Care and Use of Laboratory Animals [22] and ARRIVE guidelines. All animal protocols were approved by the Institutional Animal Care and Use Committee of Third Affiliated Hospital of Sun Yat-sen University. Fourteen-week-old male Sprague-Dawley (SD) rats were purchased from Guangdong medical laboratory animal center (Guangzhou, China). All rats were housed in a 12 h dark/light cycle with ad libitum access to food and water, 22 ± 2°C temperature, and humidity-controlled clean cages.

2.2. Rat surgical brain injury model procedures

SBI was produced according to the Loma Linda group established protocol [23,24]. Briefly, animals were anesthetized with pentobarbital sodium (60 mg/kg; Intraperitoneally). Surgery procedures were performed under aseptic conditions. Craniotomy was performed to display the right frontal lobe. The sectioned brain was then removed by making two incisions: 2 mm lateral of sagittal and 1 mm proximal of coronal planes. Hemostasis was maintained by intraoperative packing and saline irrigation, after which the skin was sutured. Sham surgery included the same surgical procedure to remove the skull while the dura-mater was kept intact.

2.3. Drugs administration

The scheme of the drug administration procedure was shown in Fig. 5. A total of 55 mice were randomly divided into the following groups: (1) SHAM = 6; (2) SBI = 7; (3) SBI + Vehicle = 6; (4) Setanaxib = 6; (5) ISRIB = 8 (4) SBI + Setanaxib = 10; (5) SBI + ISRIB = 12. PBS (0.01% DMSO) treatment serves as vehicle. Setanaxib (GKT137831) treatment, 30 mg/kg/d p.o. from 1 day before SBI to 14 days serve as positive control. Integrated stress response inhibitor, trans-ISRIB, was administrated according to the previous report with slight modification [17,25]. Briefly, 5 mg ISRIB was dissolved in 1 ml DMSO and 1 ml PEG400 (Sigma-Aldrich). Then 1.25 mg/kg ISRIB was delivered via i.p. injections one-day post-SBI for 14 days.

2.4. Immunohistochemistry

At 28 days after SBI procedures, rats were deeply anesthetized and transcardially perfused with 0.9% NaCl followed by 4% PFA in PBS. Brains were embedded in Tissue-Tek® O.C.T. Compound (Sakura Finetek USA), sectioned at a thickness of 10 μm, and captured on poly-L-lysine-coated slides. After blocking with 5% donkey serum (Jackson ImmunoResearch Laboratories, US), the sections were incubated overnight at 4 °C with the following primary antibodies: goat anti Iba1 (1:200, Wako, 011–27,991), rabbit anti ATF4(1:400, Abclonal, A0201). After washing, sections were incubated for 2 h at 37 °C with the appropriate donkey secondary antibodies conjugated with DyLight 488 or DyLight 549 (1:200, Jackson ImmunoResearch Laboratories, AB_2337273 or AB_2339165), then counterstained with 4′,6-diamidino-2-phenylindole (DAPI) for 2 min at room temperature. The stained sections were then imaged under a fluorescence microscope (Eclipse-80i, Olympus, Japan). For fluorescence quantification, images were processed for automated analysis with ImageJ, Version 1.48 (NIH).

2.5. Neurobehavioral evaluation

In this part, two blind testers performed the neurobehavioral tests below on rats in each group on the first day, the third day, the seventh day, and the fourteenth day after surgery. Any disagreement was resolved unanimously by discussion.

Modified Garcia Neurological Test:Neurologic function assessment was performed using the modified Garcia Neurological Test (GNT) [26]. (a) Spontaneous activity: rats were placed in a large cage, and observations were made on the animal's activity level for 5 min. (b) Symmetry in the limbs' movement: rats were lifted by the tails, and limb symmetry was noted. (c) Forepaw stretchability: rats were lifted by the tails and made for walking on only the forelimbs to evaluate movement on both sides. (d) Climbing experiment: the animal was placed on the 45 degrees inclined plane, and observations were made for 1 min. (e) Lateral turning: assess rat's ability to walk straight or turn to one side; (6) Tactile emission on both sides of the trunk: use a cotton swab to stimulate one side of the rat's body, and observe the difference in response on both sides of the body; (7) Tactile reflex of the tentacles on both sides: use a cotton swab to stimulate the rat's tentacles and observe the difference in response on both sides of the body. Each parameter was given ranging from 0 to 3 points, with a total score of 21 points. The higher the score, the better the function.

Balance beam experiment: The balance beam test was performed using a wooden strip with a length of 100 cm, and a width of 1.5 cm was placed between the two platforms [27]. The rat was placed in the center of the balance beam and noted when the rat stayed on. The time it took to walk to any platform to judge its balance ability. The score is 0 to 5 as follows: (a) 5 points, animal reached platform within 25 s; (b) 4 points, animal reached platform between 25 and 40 s; (c) 3 points, the animal moved halfway to a platform and stayed on the beam for at least 25 s; (d) 2 points, the animal moved less than halfway on the beam and stayed on the beam for at least 25 s; (e) 1 point, the animal did not move and stayed on the beam for 40 s; and (f) 0 points, the animal fell off the beam in less than 25 s. The higher the score, the better the function.

2.6. Cell culture, treatment, and siRNA transfection

The mouse microglial cell line BV-2 (Elabscience, EP-CL-0493) and the human microglial cell line HMC3 (ATCC, CRL-3304) were cultured

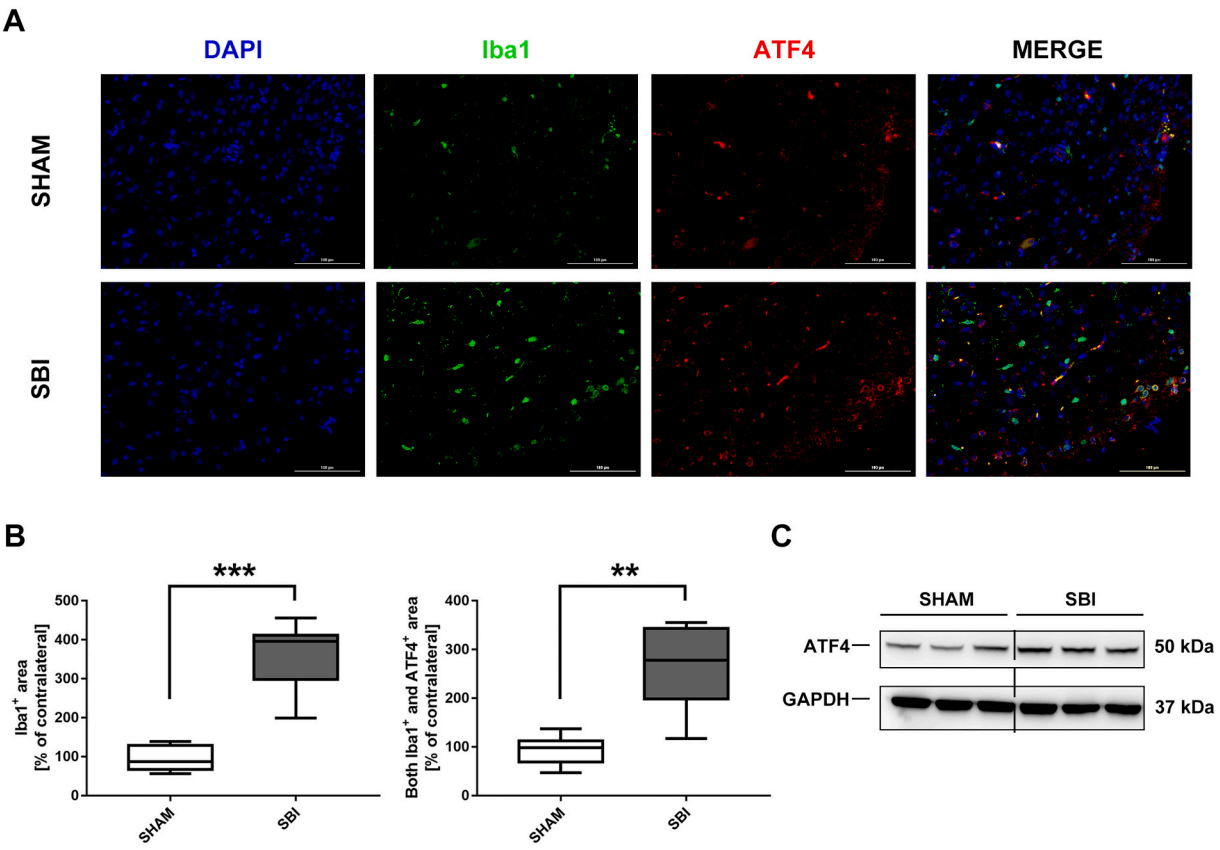

Fig. 1. Increased ATF4 expression is associated with microglia infiltration in the SBI rat model. (a) Representative image of double-immunostaining of Iba1 (green) and ATF4 (red) in the peri-resection region of the brain at 24 h after SBI application. Scale bar = 100 μm. (b) The histogram displays the fluorescence signal compared with respective controls. Values are presented as mean ± SEM of three individual experiments, ** $p < 0.01$, ***$p < 0.001$ SBI vs SHAM. (c) Western blotting showed an increased expression of ATF4 in cortex tissue after SBI injury.

in MEM containing 10% fetal bovine serum. Cells were treated with 10 nM ISRIB for six hours before treatment with lipopolysaccharide (LPS). According to manufacturer instructions, cells were transfected with 200 pmol ATF4-targeting small interfering RNA (Genechem, Shanghai) or scramble siRNA using a transfection reagent (Abclonal, RM09014) 24 h before treatment with LPS. The western blotting experiment detected the expression of ATF4 to confirm siRNA interference successfully. Cells were treated with 1 ng/ml LPS for 24 h before analysis.

2.7. Immunocytochemistry

Cells were fixed with 4% PFA for 10 min at room temperature, after blocked and permeabilized overnight with 5% donkey serum in PBS containing 0.3% Triton X-100 (Sigma-Aldrich) at 4 °C. Cells were incubated overnight at 4 °C with the following primary antibodies: rat anti CD 16/32(1:200, Abcam, ab25235), rabbit anti ATF4(1:400, Abclonal, A0201). After washing, sections were incubated for 2 h at 37 °C with the appropriate donkey secondary antibodies conjugated with DyLight 488 or DyLight 549 (Jackson ImmunoResearch Laboratories, AB_2337273 or AB_2339165), then counterstained with DAPI for 2 min at room temperature. The stained sections were then imaged under a fluorescence microscope (Eclipse-80i, Olympus, Japan).

2.8. ELISA tests

IL-6, IL-10, TGF-β, and TNF-α levels in cell culture supernatant were measured according to the manufacturer's instructions (Meimian Biotechnology, Jiangsu, China). Briefly, standards and samples were added to the micro ELISA strip-plate wells, incubated for 30 min at 37 °C, and washed five times. Add HRP-Conjugate reagent to each well except a blank well and then incubated for 30 min at 37 °C, washed five times. Chromogen Solution A and B were added and kept in the dark for 10 min at 37 °C. After adding stop solution, the absorbance of the samples was measured at 450 nm. The sample concentration was calculated according to a standard curve and then multiplied by the dilution multiplier to obtain the sample's actual concentration.

2.9. Flow cytometry

Cells were harvested and resuspended with PBS, then incubated with 10 μL anti-CD16/32-PE (eBioscience, 12–0161-82) and anti-CD 206-APC (eBioscience, 17–2061-82) antibody per 10^6 cells at room temperature for 30 min in the dark. Subsequently, cells were washed three times with PBS and resuspended for testing. The proportions of CD 16/32+ and CD 206+ cells were evaluated with a BD FACSArial Flow Cytometer. Results were analyzed by the FlowJo software program (Tree star, CA, US).

2.10. Western blotting

Brain sample tissues or cells were harvested and homogenized in Ripa lysis buffer (Beyotime, P0013B). After homogenization, samples

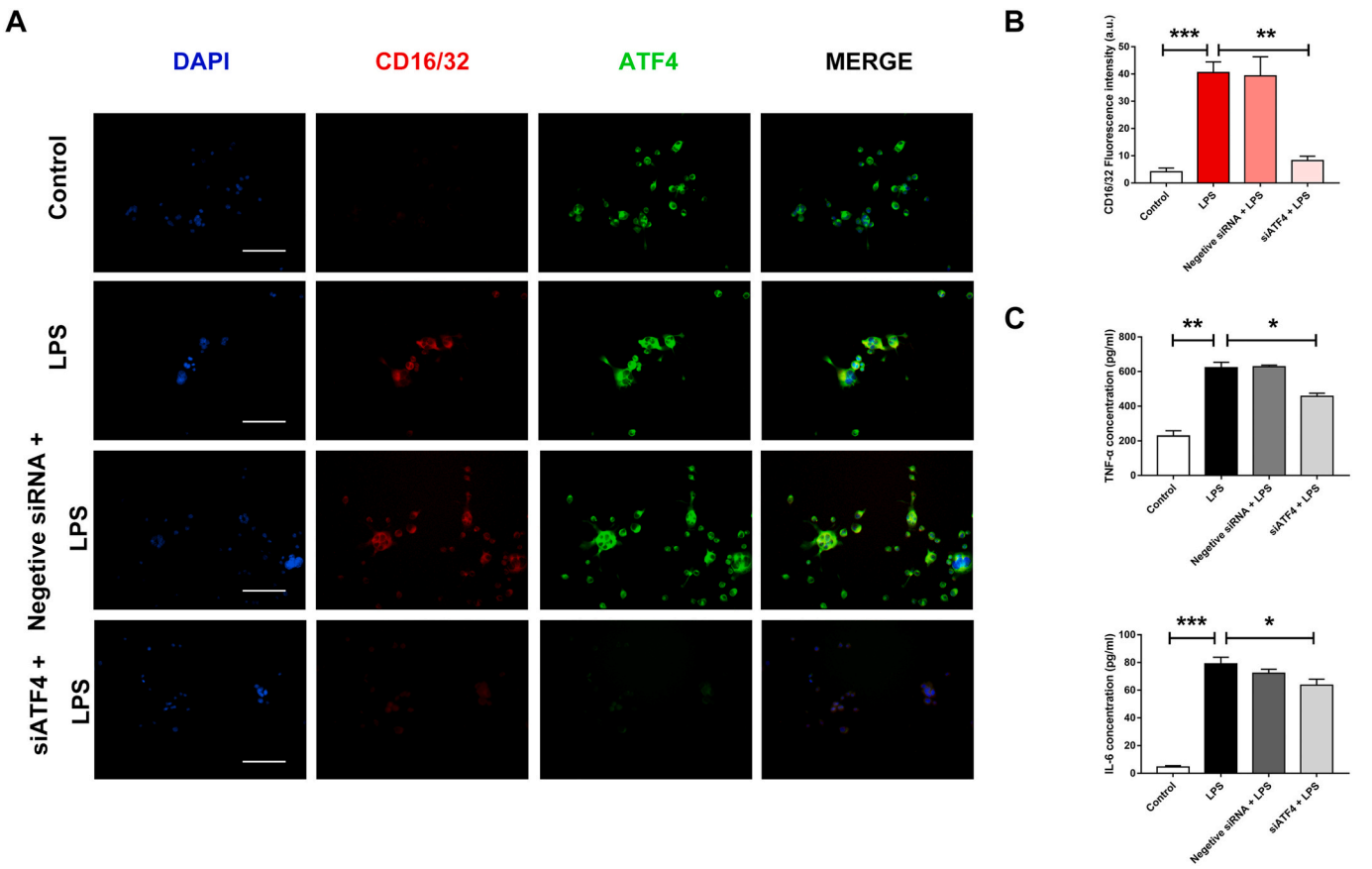

Fig. 2. ATF4-dependent LPS-mediated microglia M1 phenotype activation. (a) Representative images of double-immunostaining of ATF4 (green) and CD16/32 (red) in BV2 cells after LPS treatment (1 ng/ml for 24 h) showed the knockdown of ATF4 effectively inhibit the expression of CD16/32. Scale bar = 50 μm. (b) Fluorescence intensity analysis of CD16/32 in BV2 cells from different groups. (c) ELISA analysis found decreased TNFα and IL-6 protein concentrations in the supernatants derived from BV2 cells treated with ATF4 siRNA. Values are presented as mean ± SEM of three individual experiments. *$p < 0.05$, **$p < 0.01$, ***$p < 0.001$ vs. control group.

were centrifuged at 12,000*g* at 4 °C for 10 min. The supernatants were collected, and the samples' protein concentration was determined using a detergent compatibility assay. Samples were loaded on 10% precast gel (Bio-Rad Laboratories, Hercules, CA), and blocked with 5% skim milk at room temperature for 1 h, and then incubated with primary antibodies at 4 °C overnight: ATF4 (Abclonal, 1:1000, A0201), NOX4 (Abclonal, 1:1000, A2201). Samples were rinsed three times with PBS solution containing 0.1% Tween-20 (PBST) and incubated with secondary antibodies (anti-Mouse/Rabbit, Southern biotech, 1:10000, AB_2650510) for 1 h at room temperature. Developing was performed with Immobilon Western Chemilum HRP Substrate (Millipore, WBKLS0500) for 1 min. Chemiluminescent images were analyzed with a Fujifilm LAS-3000 Luminescent Image Analyzer system. The band density for each sample was determined relative to β-actin or GAPDH.

2.11. Statistical analysis

All statistical analyses were performed on SPSS v.20.0 for Windows (IBM Japan, Ltd., Tokyo, Japan) and GraphPad Prism 7 (GraphPad Software). The student's *t*-test was used for pairwise comparison. Means were compared groups by one-way ANOVA with post hoc Bonferroni's multiple comparisons. All data presented are means ± SEM, and *P* values <0.05 were considered statistically significant.

3. Results

3.1. Increased microglia infiltration and ATF4 expression in the surgical margin of cortex

The inducible ISR transcriptional factor ATF4 plays a vital role in regulating cellular stress along with the pathogenesis of neurodegeneration diseases [28]. We first tested the contribution of endogenic ATF4 in the surgical margin of the cortex. Immunostaining results showed that Iba1+ microglia infiltration was highly detected in the excision margin of the SBI group while compared to the sham group (Fig. 1a). Double immunostaining revealed that ATF4 was found localized mainly within the cytoplasm of Iba1^{+} microglia (Fig. 1a, b). Moreover, the protein expression level of ATF4 was significantly increased in the SBI cortex tissue compared to the sham group (Fig. 1c). Together, these results are consistent with the known role of ATF4 in controlling neuronal cell death after brain injury [29]. Co-expression of ATF4 and Iba1 indicates that ISR may also regulate infiltrated microglia within the SBI margin of the cortex.

3.2. Knockdown of ATF4 inhibited the activation of LPS-mediated microglial M1 phenotype

Given that the effects of indirect inhibition of ATF4 signaling

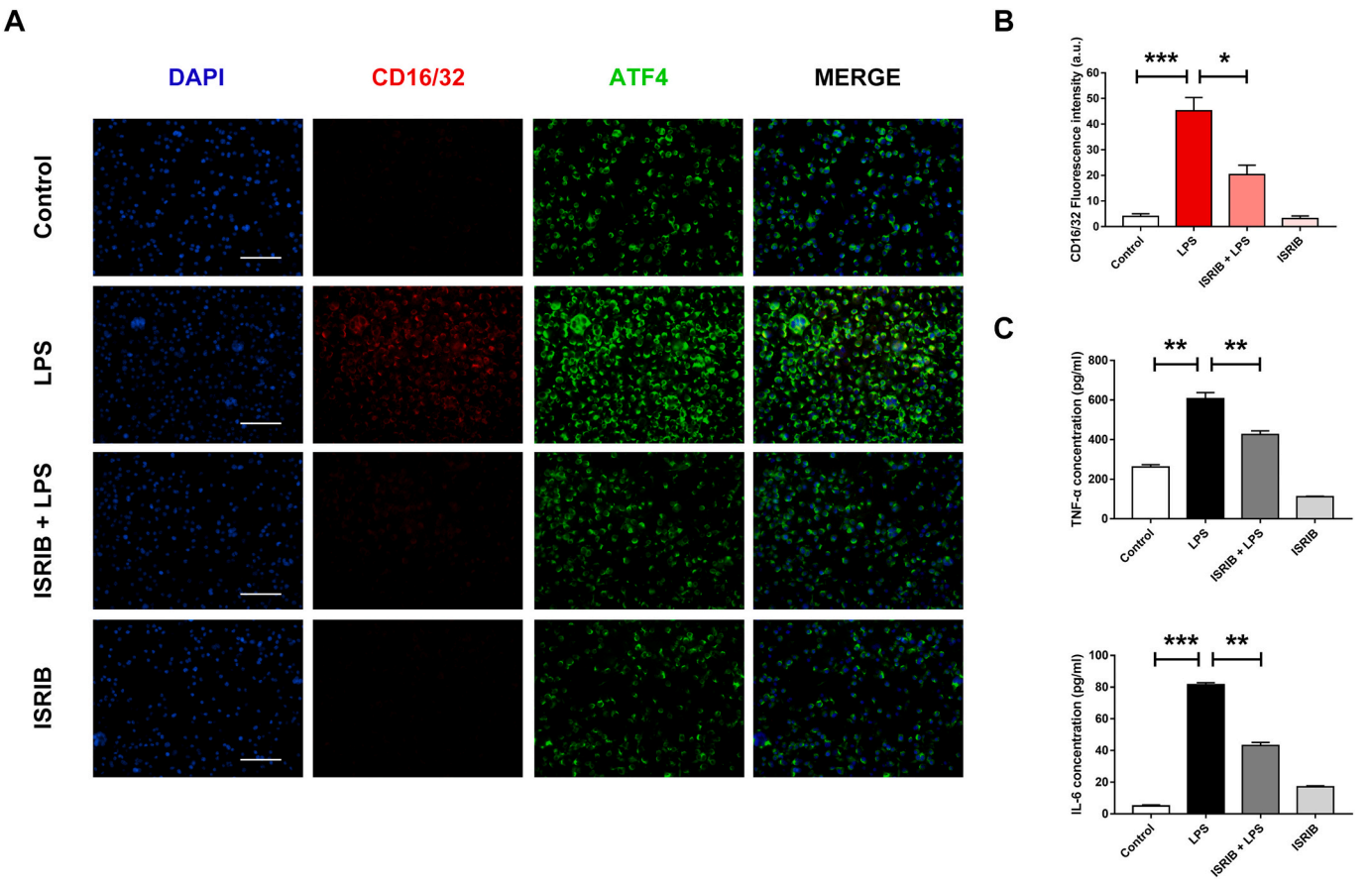

Fig. 3. ISRIB reduces LPS-stimulated microglia M1 phenotype differentiation and suppresses the production of proinflammatory cytokines. (a) Representative images of double-immunostaining of ATF4 (green) and CD16/32 (red) in BV2 cells after LPS treatment (1 ng/ml for 24 h) showed ISRIB suppresses the expression of CD16/32. Scale bar = 50 μm. (b) Fluorescence intensity analysis of CD16/32 in BV2 cells from different groups. (c) ELISA analysis quantified a decreased amount of TNFα and IL-6 proteins in the BV2 culture supernatant after treating with ISRIB. Values are presented as mean ± SEM of three individual experiments. $^{**}p < 0.01$, $^{***}p < 0.001$ vs. control group.

pathway had been shown to suppress LPS-induced microglia activation [19], we therefore examined the direct regulation effect of ATF4 on the LPS-stimulated microglial activation. By performing immunofluorescence, we found that knockdown of ATF4 mRNA expression in BV-2 cells with siRNA significantly attenuated M1 phenotype activation after LPS treatment (Fig. 2a). The fluorescence intensity of CD16/32 was decreased by 28.2 ± 4.1% in cells pretreated with siATF4 compared to cells treated with LPS alone (Fig. 2a, b). Furthermore, the secreted protein levels of TNF-α and IL-6 with LPS treatment were significantly reduced by 26.0 ± 3.4% and 18.7 ± 1.2%, respectively, in cells pretreated with siATF4 (Fig. 2b). These results suggested that ATF4 involves in regulating LPS-induced microglial M1 phenotype activation.

3.3. ISRIB suppressed LPS-stimulated microglial M1 polarization

A previous study suggested that ISRIB inhibits PERK-dependent inflammation in astrocytes [30]. Next, BV-2 cells were exposed to LPS with or without ISRIB. Interestingly, ISRIB treatment significantly decreased LPS-stimulated activation of CD16/32 on microglia (Fig. 3a, b). We also observed a significant decrease in ATF4 expression in companies with ISRIB treatment. We found that treatment with ISRIB alone showed no difference in CD16/32 activation. Of note, ISRIB exerted a significant attenuated effect on TNF-α and IL-6 secretion (Fig. 3c). Based on the above findings, we concluded that ISRIB exhibits suppressive effects on LPS-stimulated microglial M1 polarization via inhibiting the ISR signaling pathway.

3.4. ISRIB promoted a switch toward the M2 phenotype and inhibited the intracellular NOX4 expression

A previous study suggested that chronic ISR activation contributes to upregulated M1/M2 ratios and related inflammation [31]. The FACS analyses showed that administration of ISRIB before LPS treatment resulted in a significant decrease of the proportion of CD16/32-positive cells (From 60.8 ± 12.7% to 29.1 ± 5.8%, Q3(UR) and Q4(LR), Fig. 4a). On contrary, the proportion of CD206-positive cells was increased from 0.5% ± 0.2% to 39.7 ± 11.8% (Q1(UL) and Q3(UR), Fig. 4a). Surprisingly, 29.5% ± 8.4% of the cells show both CD16/32 and CD206 positive (Q3(UR), Fig. 4a). ISRIB also increased the productions of anti-inflammatory cytokine IL-10 and TGF-β under LPS treatment (Fig. 4c). Surprisingly, ISRIB alone slightly reduced IL-10 or TGF-β protein production. These results indicate that ISRIB may promote the M1 to M2 phenotype transition under an inflammatory microenvironment.

We then explore the preliminary mechanism of ISRIB promoting the M1 to M2 phenotype conversion under an inflammatory microenvironment. NADPH oxidases 4 (NOX4) has been found to regulate ISR signaling upon cellular stress [32]. NOXs inhibition has been shown to favors M2 microglia polarization [33]. We therefore wonder whether

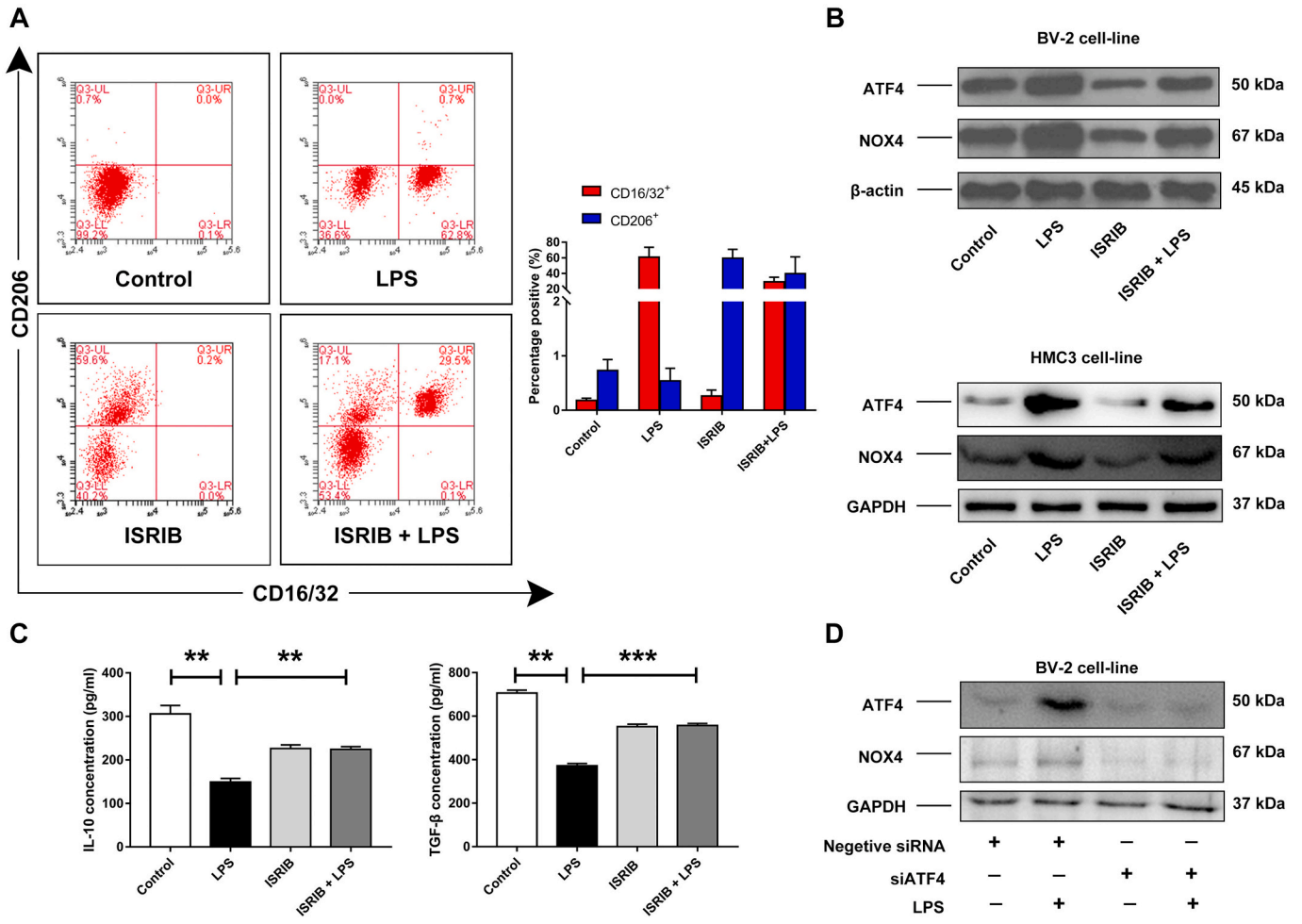

Fig. 4. ISRIB promotes a switch toward the M2 phenotype by suppressing NOX4 expression. (a) Representative result of FACS analyses the double-staining of CD16/32 and CD206 in BV2 cells after LPS or ISRIB treatment. (b) Western blotting showed decreased ATF4 and NOX4 expression after treating with ISRIB in BV2 or HMC3 cell line. (c) ELISA analysis quantified an increased amount of IL-10 and TGF-β proteins in the BV2 culture supernatant after treating with ISRIB. (c) Western blotting showed a decreased expression of NOX4 expression after targeting ATF4. Values are presented as mean ± SEM of three individual experiments. $^{**}p < 0.01$, $^{***}p < 0.001$ vs. control group.

ISRIB can regulate NOX4 protein expression during M1 to M2 transition. As shown in Fig. 4b, ISRIB significantly reduced ATF4 or NOX4 protein expression in BV-2 cells. In addition, this effect was also detectable in human HMC3 microglia cells (Fig. 4b). To further verify the role of ATF4 in mediating NOX4 expression, we found that ATF4 siRNA robustly prevented NOX4 protein expression (Fig. 4d). These data suggested that ISRIB promotes M1 to M2 phenotype conversion under inflammatory microenvironment and may regulate intracellular NOX4 expression.

3.5. The administration of ISRIB Reducesed ATF4 expression and attenuated microglia infiltration in the SBI rat model

A very recent study showed that ISR is involved in the glia cells' differentiation and maturation [34]. We therefore further investigated the anti-inflammatory effect of ISRIB in vivo. It was evident that there was a significant reduction in the microglia infiltration or ATF4 expression in the ISRIB+SBI group surgical margin, compared to SBI or SBI + Vehicle group, respectively (Fig. 6a, b). Notably, when rats were pretreated Setanaxib, a dual NOX1/4 inhibitor, microglia infiltration or ATF4 expression was blocked (Fig. 6a, b), indicating possible positive feedback between ATF4 and NOX4 [32]. These findings inlined with the above in vitro results and indicated that the administration of ISRIB could impede neuroinflammation via attenuating M1 microglia infiltration in the SBI rat model.

3.6. ISRIB modulated the neurobehavioral outcomes in the SBI neuroinflammatory microenvironment

Persistent neurobehavioral deficits after brain injury were considered relevant to a chronic neuroinflammatory microenvironment [35]. Next, we examined neurological scoring that responds to ISRIB following SBI. As shown in Fig. 7a, Setanaxib or ISRIB treatment significantly improved GNT following SBI injury on days 7 and 14 ($p < 0.05$, respectively). In addition, the beam balance test in rats of SBI or SBI + Vehicle group was significantly lower than that along with Setanaxib or ISRIB treatment at days 3, 7, and 14 post-injury, respectively ($p < 0.05$, Fig. 7b), indicating ISRIB can improve both the neurological and neuromotor function under the SBI neuroinflammatory microenvironment.

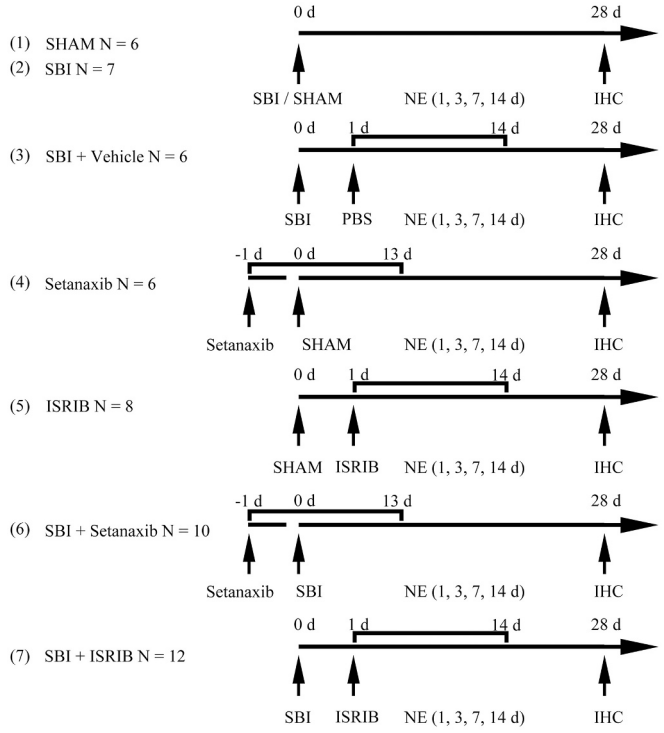

Fig. 5. The scheme of the drug administration procedure. PBS (0.01% DMSO) treatment serves as Vehicle. Setanaxib (GKT137831) 30 mg/kg/d p.o. 1 day before SBI and for 14 days. *Trans*-ISRIB 1.25 mg/kg was delivered via i.p. injections one day post-SBI for 14 days. NE, Neurobehavioral Evaluation.

4. Discussion

Here we demonstrate that the ISR transcription factor ATF4 mediates the LPS-induced M1 microglia polarization in vitro. Inhibition of the ISR with small molecule ISRIB can promote an M1/M2 switching and downregulate the intracellular NOX4 expression in microglia. Remarkably, ISRIB suppressed the infiltration of microglia and improved neurobehavioral outcomes in the SBI animal model. These data suggested that ISRIB would be a promising candidate for attenuating the neuroinflammatory microenvironment following SBI (Fig. 8).

Previous studies have reported that an essential role of neuroinflammation in SBI, defined as BBB disruption, leukocyte infiltration, microglia activation, and presenting inflammatory cytokines in the brain resection margin [36]. The inflammation cascade reaches a peak 24 h after SBI [7] and develops into chronic neuroinflammation further [37]. Targeting acute neuroinflammation showed a benefit of neurological outcomes in SBI [38]. However, attempts to intervene in the acute inflammatory response after brain injury may be difficult for preclinical/clinical practice. Besides, ISRIB suppresses the ISR with a bell-shaped window during activation [39]. We therefore applied the ISRIB treatment at the acute-chronic period (1-day post-SBI). Our results demonstrate that a supplement of ISRIB could suppress microglia infiltration after 28 days of observation, thereby offers an alternative target for treating acute-chronic neuroinflammation resulting from SBI.

Microglia tends to remove debris to protect the neurons [40] and switch between M1/M2 polarization to influence the neurotrophic growth factor expression in CNS [41]. Addressing microglia activation can promote an optimal functional recovery after brain injury [42]. ATF4 signaling pathway plays a novel role in the differentiation and cellular stress response in microglia [43]. Notably, the ATF4 signaling pathway is associated with inflammasome activation and inflammatory cytokines production in LPS-stimulated microglia [44]. Our results showed that ATF4 expression was upregulated in the brain resection margin and co-expressed with Iba1+ microglia after SBI. We further demonstrated that targeting ATF4 via siRNA could suppress the LPS-mediated M1 activation and proinflammatory cytokines secretion in vitro. ATF4 may activate transcriptional reprogramming for regulating the production of proinflammatory cytokines [44]. However, whether these proinflammatory cytokines mRNA contain the short inhibitory upstream open reading frames essential to ATF4 binding sites still needed to be determined [16].

Neuronal ER stress pathway p-eIF2α/ATF4/CHOP had been shown linked to neuroinflammation and neuronal cell death in TBI [45]. Our results indicated that ISRIB significantly attenuates the microglia infiltration within the surgical margin, which extended our understanding of ISR axis involvement in the neuroinflammation development following SBI. A previous study suggested that ISRIB actives eIF2B to counteract eIF2 phosphorylation, thus downregulate ATF4 expression in brain diseases [46]. ISRIB also mediated neuronal survival in neurodegenerative disease [47]. Interestingly, we found that ISRIB promotes a switch toward the M2 microglia phenotype under an inflammatory microenvironment. It has been reported that inhibiting the eIF2α signaling pathway is associated with promoting M2 macrophage polarization in chronic inflammation [48]. Since ISRIB can restores protein translation under stress conditions [49], some specific proteins, including TREM2, may be the effector in favor of M2 microglia polarization [50]. Considering ISRIB suppressed PERK/ eIF2α-mediated inflammatory gene expression, the memory-enhancing effect of ISRIB [51] might strengthen the possibility of favorable treatment for SBI.

NADPH oxidase enzymes were responsible for the imbalance of oxidative stress in brain injury [52,53]. Antioxidant therapies with inhibition of NOXs can reduce neuroinflammation in both SBI or TBI animal models [54–56]. Studies have revealed that deletion of NOX4 can improve neurological outcomes, ischemic damage, and chronic neurodegeneration in TBI [57–59]. It has been reported that NOX4-derived ROS can activate the PERK/eIF-2α/ATF4 signaling pathway under stress conditions [60]. In this study, we found that NOX4 expression was decreased after ATF4-targeting or ISRIB treatment. We also tested the anti-inflammatory effect of inhibition of NOX1/4 in vivo, which in line with the previous result that Setanaxib has anti-inflammatory effects on the microglia [61]. Further studies are needed to elucidate the connection between the ISR and NOX4 under the neuroinflammatory microenvironment.

There are limitations to the study. First, the upstream signaling, four eIF-2α kinases (HRI, PAR, PERK, GCN2) activation should be detected in the SBI model to validate the involvement of ISR in chronic neuroinflammation [62]. Second, the downstream signaling protein CHOP can be tested to determining whether CHOP may lead to the activation of the inflammasome during SBI development [63]. Third, considering PEG400 can be efficiently uptake and accumulated by microglia, further studies still need to address whether PEG400 have modification effects on microglia activation.

In conclusion, ISRIB significantly promotes microglial M1 to M2 phenotype switching under an inflammatory microenvironment. This effect is associated with the downregulation of NOX4 protein expression in microglia. ISRIB also suppressed the infiltration of microglia and improved neurobehavioral outcomes following SBI injury (Fig. 8). These data suggest that targeting ISR via ISRIB would be a potential therapeutic agent for treating neuroinflammation resulting from SBI.

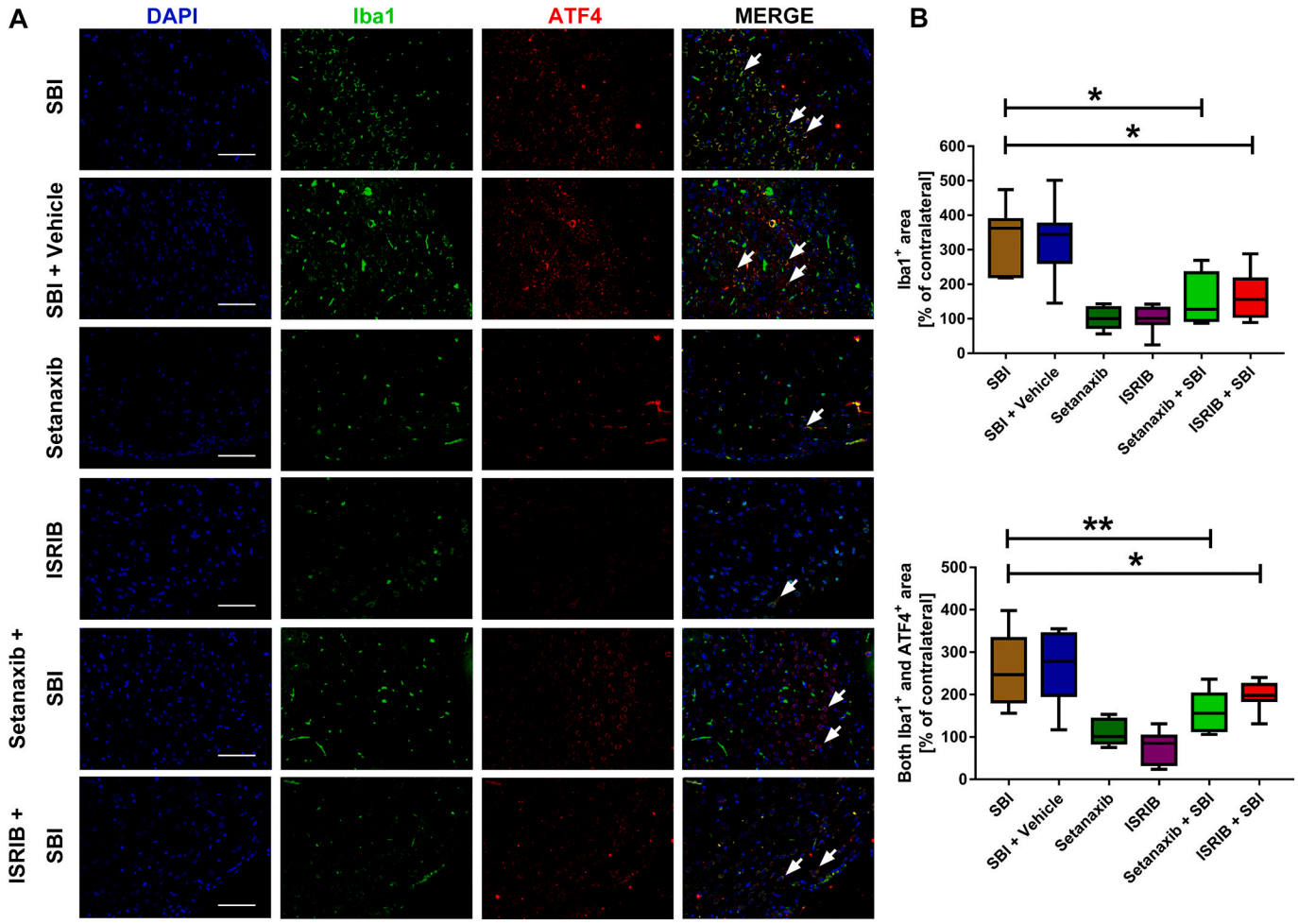

Fig. 6. Administration of ISRIB reduces the expression of ATF4 and microglia infiltration in the SBI rat model. (a) Representative images of immunohistochemistry stained peri-resection region of the brain from SBI, SBI + Vehicle, Setanaxib, ISRIB, Setanaxib + SBI, and ISRIB groups. ISRIB treatment significantly reduces ATF4 expression and prevents microglia infiltration (DAPI, blue; Iba1, green; ATF4, red; Scale bar = 50 μm.). (b) The histogram displays the fluorescence signal compared with respective controls. Values are presented as mean ± SEM of three individual experiments, ** $p < 0.01$, ***$p < 0.001$ vs SBI.

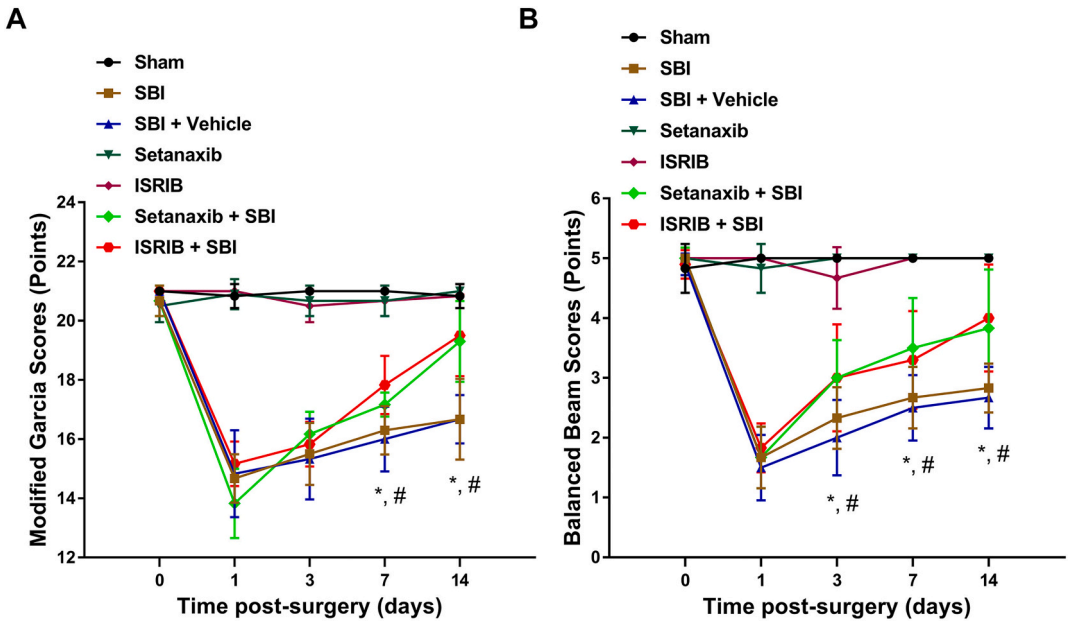

Fig. 7. The supplement of ISRIB improves the neurobehavioral outcomes in the SBI rat model. Setanaxib or ISRIB alone treatment show no adverse effect on neurobehavioral outcomes compared to the SHAM group. (a) Compared to SBI or Vehicle group, both Setanaxib and ISRIB improved GNT at days 7 and 14 post-injury. *$p < 0.05$ vs. SBI, #$p < 0.05$ vs. SBI + Vehicle. (b) The balance on a beam was assessed over 14 days post-injury period. Compared to SBI or Vehicle group, both Setanaxib and ISRIB improved balance beam scores on day 3, day 7, and day 14 after injury. *$p < 0.05$ vs. SBI, #$p < 0.05$ vs. SBI + Vehicle.

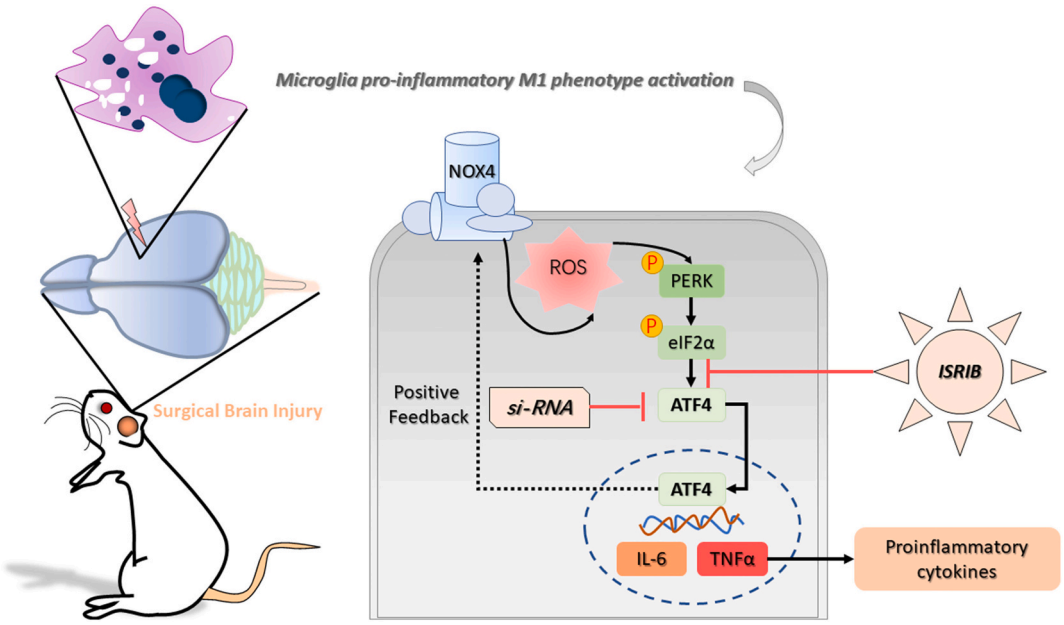

Fig. 8. Schematic diagram of the anti-neuroinflammation effect of ISRIB in SBI-mediated induction of microglia ATF4 expression and M1 phenotype activation. SBI induces NAPDH oxidase 4-related intracellular ROS production with downstream activation of the integrated stress response eIF2α/ATF4 pathway, which resulted in microglia proinflammatory M1 phenotype activation. Moreover, ATF4 also promotes the transcription of the NOX4, which may serve as positive feedback. ISRIB may modulate microglia toward a lower M1 phenotype activation and higher M2 phenotype differentiation in the SBI rat model, which leads to decreased production of the proinflammatory cytokines and improvement of neurological outcomes.

Author contributions

Tc.H., L.l., and Sh.J. designed the work, performed data analysis, wrote, and revised the manuscript; C.C. and Hy.H. performed in vitro experiments. Cf.L. and Ws.L. participated in guiding and conducting in vivo experiments. H.W. And L.Z. reviewed the study proposal, extracted data, and contributed to statistical analysis; K.W. and Y.G. analyzed the data, supervised the project, reviewed and edited the manuscript. All authors have read and approved the final manuscript.

Conflicts of interest

The authors declare no conflicts of interest.

Acknowledgments

This research was supported by grants from the Key Program of Natural Science Foundation of Guangdong Province, China (2018B0303110014); National Natural Science Foundation of China (81772368); and Key-Area Research and Development Program of Guangdong Province (2020B090924004). Data can be accessed by contacting the corresponding authors.

References

[1] P. Sherchan, C.H. Kim, J.H. Zhang, Surgical brain injury and edema prevention, Acta Neurochir. Suppl. 118 (2013) 129–133.
[2] O. Akyol, P. Sherchan, G. Yilmaz, C. Reis, W.M. Ho, Y. Wang, et al., Neurotrophin-3 provides neuroprotection via TrkC receptor dependent pErk5 activation in a rat surgical brain injury model, Exp. Neurol. 307 (2018) 82–89.
[3] M. Frontczak-Baniewicz, S.J. Chrapusta, D. Sulejczak, Long-term consequences of surgical brain injury - characteristics of the neurovascular unit and formation and demise of the glial scar in a rat model, Folia Neuropathol. 49 (2011) 204–218.
[4] D. Sulejczak, S.J. Chrapusta, W. Kozlowski, M. Frontczak-Baniewicz, Surgical injury-induced early neocortical microvascular changes and characteristics of the cells populating the peri-lesion zone, Acta Neurobiol. Exp. 76 (2016) 125–141.
[5] J.D. Cherry, J.A. Olschowka, M.K. O'Banion, Neuroinflammation and M2 microglia: the good, the bad, and the inflamed, J. Neuroinflammation 11 (2014) 98.
[6] L. Huang, H. Tang, P. Sherchan, C. Lenahan, W. Boling, J. Tang, et al., The activation of phosphatidylserine/CD36/TGF-beta1 pathway prior to surgical brain injury attenuates neuroinflammation in rats, Oxidative Med. Cell. Longev. 2020 (2020) 4921562.
[7] L. Huang, P. Sherchan, Y. Wang, C. Reis, R.L. Applegate 2nd, J. Tang, et al., Phosphoinositide 3-kinase gamma contributes to neuroinflammation in a rat model of surgical brain injury, J. Neurosci. 35 (2015) 10390–10401.
[8] M.L. James, J.M. Komisarow, H. Wang, D.T. Laskowitz, Therapeutic development of apolipoprotein E Mimetics for acute brain injury: augmenting endogenous responses to reduce secondary injury, Neurotherapeutics 17 (2020) 475–483.
[9] N. Zagzoog, K.K. Reddy, Modern brain retractors and surgical brain injury: a review, World Neurosurg. 142 (2020) 93–103.
[10] E.E. Nagy, A. Frigy, J.A. Szasz, E. Horvath, Neuroinflammation and microglia/macrophage phenotype modulate the molecular background of post-stroke depression: a literature review, Exp. Therap. Med. 20 (2020) 2510–2523.
[11] C. Zhao, Y. Deng, Y. He, X. Huang, C. Wang, W. Li, Decreased level of exosomal miR-5121 released from microglia suppresses neurite outgrowth and synapse recovery of neurons following traumatic brain injury, Neurotherapeutics (2021 Jan 21), https://doi.org/10.1007/s13311-020-00999-z.
[12] W. Zhang, T. Tian, S.X. Gong, W.Q. Huang, Q.Y. Zhou, A.P. Wang, et al., Microglia-associated neuroinflammation is a potential therapeutic target for ischemic stroke, Neural Regen. Res. 16 (2021) 6–11.
[13] M. Frontczak-Baniewicz, D. Sulejczak, J. Andrychowski, M. Gewartowska, M. Laure-Kamionowska, W. Kozlowski, Morphological evidence of the beneficial role of immune system cells in a rat model of surgical brain injury, Folia Neuropathol. 51 (2013) 324–332.
[14] Q. Chen, L. Xu, T. Du, Y. Hou, W. Fan, Q. Wu, et al., Enhanced expression of PD-L1 on microglia after surgical brain injury exerts self-protection from inflammation and promotes neurological repair, Neurochem. Res. 44 (2019) 2470–2481.
[15] Y. Tao, L. Li, B. Jiang, Z. Feng, L. Yang, J. Tang, et al., Cannabinoid receptor-2 stimulation suppresses neuroinflammation by regulating microglial M1/M2 polarization through the cAMP/PKA pathway in an experimental GMH rat model, Brain Behav. Immun. 58 (2016) 118–129.
[16] M. Costa-Mattioli, P. Walter, The integrated stress response: from mechanism to disease, Science 368 (6489) (2020 Apr 24) eaat5314.
[17] A. Chou, K. Krukowski, T. Jopson, P.J. Zhu, M. Costa-Mattioli, P. Walter, et al., Inhibition of the integrated stress response reverses cognitive deficits after traumatic brain injury, Proc. Natl. Acad. Sci. U. S. A. 114 (2017). E6420-E6.
[18] L. Romero-Ramirez, M. Nieto-Sampedro, M.A. Barreda-Manso, Integrated stress response as a therapeutic target for CNS injuries, Biomed. Res. Int. 2017 (2017) 6953156.
[19] H. Hara, D. Kimoto, M. Kajita, C. Takada, T. Kamiya, T. Adachi, Apomorphine prevents LPS-induced IL-23 p19 mRNA expression via inhibition of JNK and ATF4 in HAPI cells, Eur. J. Pharmacol. 795 (2017) 108–114.
[20] Z. Lu, Z. Wang, L. Yu, Y. Ding, Y. Xu, N. Xu, et al., GCN2 reduces inflammation by p-eIF2alpha/ATF4 pathway after intracerebral hemorrhage in mice, Exp. Neurol. 313 (2019) 16–25.
[21] M.M. Oliveira, M.V. Lourenco, F. Longo, N.P. Kasica, W. Yang, G. Ureta, et al., Correction of eIF2-dependent defects in brain protein synthesis, synaptic plasticity, and memory in mouse models of Alzheimer's disease, Sci. Signal. 14 (2021).
[22] Guide for the Care and Use of Laboratory Animals. Washington (DC)1996.
[23] V. Jadhav, M. Yamaguchi, A. Obenaus, J.H. Zhang, Matrix metalloproteinase inhibition attenuates brain edema after surgical brain injury, Acta Neurochir. Suppl. 102 (2008) 357–361.
[24] T.P. Bravo, G.A. Matchett, V. Jadhav, R.D. Martin, A. Jourdain, A. Colohan, et al., Role of histamine in brain protection in surgical brain injury in mice, Brain Res. 1205 (2008) 100–107.
[25] M. Halliday, H. Radford, Y. Sekine, J. Moreno, N. Verity, J. le Quesne, et al., Partial restoration of protein synthesis rates by the small molecule ISRIB prevents neurodegeneration without pancreatic toxicity, Cell Death Dis. 6 (2015), e1672.
[26] J.H. Garcia, S. Wagner, K.F. Liu, X.J. Hu, Neurological deficit and extent of neuronal necrosis attributable to middle cerebral artery occlusion in rats. Statistical validation, Stroke 26 (1995) 627–634 (discussion 35).
[27] U. Scherbel, R. Raghupathi, M. Nakamura, K.E. Saatman, J.Q. Trojanowski, E. Neugebauer, et al., Differential acute and chronic responses of tumor necrosis factor-deficient mice to experimental brain injury, Proc. Natl. Acad. Sci. U. S. A. 96 (1999) 8721–8726.
[28] I.M.N. Wortel, L.T. van der Meer, M.S. Kilberg, F.N. van Leeuwen, Surviving stress: modulation of ATF4-mediated stress responses in normal and malignant cells, Trends Endocrinol. Metab. 28 (2017) 794–806.
[29] J.M. Farook, J. Shields, A. Tawfik, S. Markand, T. Sen, S.B. Smith, et al., GADD34 induces cell death through inactivation of Akt following traumatic brain injury, Cell Death Dis. 4 (2013), e754.
[30] L.N. Guthrie, K. Abiraman, E.S. Plyler, N.T. Sprenkle, S.A. Gibson, B.C. McFarland, et al., Attenuation of PKR-like ER kinase (PERK) signaling selectively controls endoplasmic reticulum stress-induced inflammation without compromising immunological responses, J. Biol. Chem. 291 (2016) 15830–15840.
[31] A. Khalyfa, Z. Qiao, A. Gileles-Hillel, A.A. Khalyfa, M. Akbarpour, B. Popko, et al., Activation of the integrated stress response and metabolic dysfunction in a murine model of sleep apnea, Am. J. Respir. Cell Mol. Biol. 57 (2017) 477–486.
[32] C.X. Santos, A.D. Hafstad, M. Beretta, M. Zhang, C. Molenaar, J. Kopec, et al., Targeted redox inhibition of protein phosphatase 1 by Nox4 regulates eIF2alpha-mediated stress signaling, EMBO J. 35 (2016) 319–334.
[33] S. Bermudez, G. Khayrullina, Y. Zhao, K.R. Byrnes, NADPH oxidase isoform expression is temporally regulated and may contribute to microglial/macrophage polarization after spinal cord injury, Mol. Cell. Neurosci. 77 (2016) 53–64.
[34] L.M. Roth, B. Zidane, L. Festa, R. Putatunda, M. Romer, H. Monnerie, et al., Differential effects of integrase strand transfer inhibitors, elvitegravir and raltegravir, on oligodendrocyte maturation: a role for the integrated stress response, Glia. 69 (2021) 362–376.
[35] S.L. Sell, K. Johnson, D.S. DeWitt, D.S. Prough, Persistent behavioral deficits in rats after parasagittal fluid percussion injury, J. Neurotrauma 34 (2017) 1086–1096.
[36] A. Hyong, V. Jadhav, S. Lee, W. Tong, J. Rowe, J.H. Zhang, et al., Rosiglitazone, a PPAR gamma agonist, attenuates inflammation after surgical brain injury in rodents, Brain Res. 1215 (2008) 218–224.
[37] A.I. Faden, D.J. Loane, Chronic neurodegeneration after traumatic brain injury: Alzheimer disease, chronic traumatic encephalopathy, or persistent neuroinflammation? Neurotherapeutics 12 (2015) 143–150.
[38] F.F. Xu, S. Sun, A.S. Ho, D. Lee, K.M. Kiang, X.Q. Zhang, et al., Effects of progesterone vs. dexamethasone on brain oedema and inflammatory responses following experimental brain resection, Brain Inj. 28 (2014) 1594–1601.
[39] H.H. Rabouw, M.A. Langereis, A.A. Anand, L.J. Visser, R.J. de Groot, P. Walter, et al., Small molecule ISRIB suppresses the integrated stress response within a defined window of activation, Proc. Natl. Acad. Sci. U. S. A. 116 (2019) 2097–2102.
[40] M.R. Kotter, C. Stadelmann, H.P. Hartung, Enhancing remyelination in disease–can we wrap it up? Brain 134 (2011) 1882–1900.
[41] H.S. Suh, M.L. Zhao, L. Derico, N. Choi, S.C. Lee, Insulin-like growth factor 1 and 2 (IGF1, IGF2) expression in human microglia: differential regulation by inflammatory mediators, J. Neuroinflammation 10 (2013) 37.
[42] D.J. Loane, K.R. Byrnes, Role of microglia in neurotrauma, Neurotherapeutics 7 (2010) 366–377.
[43] A. Juknat, M. Pietr, E. Kozela, N. Rimmerman, R. Levy, G. Coppola, et al., Differential transcriptional profiles mediated by exposure to the cannabinoids cannabidiol and Delta9-tetrahydrocannabinol in BV-2 microglial cells, Br. J. Pharmacol. 165 (2012) 2512–2528.
[44] T. Inoue, H. Yamakage, M. Tanaka, T. Kusakabe, A. Shimatsu, N. Satoh-Asahara, Oxytocin suppresses inflammatory responses induced by lipopolysaccharide through inhibition of the eIF-2-ATF4 pathway in mouse microglia, Cells. 8 (2019).
[45] S. Liu, R. Jin, A.Y. Xiao, R. Chen, J. Li, W. Zhong, et al., Induction of neuronal PI3Kgamma contributes to endoplasmic reticulum stress and long-term functional impairment in a murine model of traumatic brain injury, Neurotherapeutics 16 (2019) 1320–1334.
[46] Y.L. Wong, L. LeBon, R. Edalji, H.B. Lim, C. Sun, C. Sidrauski, The small molecule ISRIB rescues the stability and activity of vanishing white matter disease eIF2B mutant complexes, eLife. 7 (2018).
[47] R. Bugallo, E. Marlin, A. Baltanas, E. Toledo, R. Ferrero, R. Vinueza-Gavilanes, et al., Fine tuning of the unfolded protein response by ISRIB improves neuronal survival in a model of amyotrophic lateral sclerosis, Cell Death Dis. 11 (2020) 397.
[48] W. Cao, T. Zhang, R. Feng, T. Xia, H. Huang, C. Liu, et al., Hoxa5 alleviates obesity-induced chronic inflammation by reducing ER stress and promoting M2 macrophage polarization in mouse adipose tissue, J. Cell. Mol. Med. 23 (2019) 7029–7042.
[49] A.A. Anand, P. Walter, Structural insights into ISRIB, a memory-enhancing inhibitor of the integrated stress response, FEBS J. 287 (2020) 239–245.
[50] J.B. Ruganzu, Q. Zheng, X. Wu, Y. He, X. Peng, H. Jin, et al., TREM2 overexpression rescues cognitive deficits in APP/PS1 transgenic mice by reducing neuroinflammation via the JAK/STAT/SOCS signaling pathway, Exp. Neurol. 336 (2021) 113506.
[51] J.C. Tsai, L.E. Miller-Vedam, A.A. Anand, P. Jaishankar, H.C. Nguyen, A.R. Renslo, et al., Structure of the nucleotide exchange factor eIF2B reveals mechanism of memory-enhancing molecule, Science 359 (2018).

[52] S.J. Cooney, S.L. Bermudez-Sabogal, K.R. Byrnes, Cellular and temporal expression of NADPH oxidase (NOX) isotypes after brain injury, J. Neuroinflammation 10 (2013) 155.
[53] M.W. Ma, J. Wang, Q. Zhang, R. Wang, K.M. Dhandapani, R.K. Vadlamudi, et al., NADPH oxidase in brain injury and neurodegenerative disorders, Mol. Neurodegener. 12 (2017) 7.
[54] E.D. Hall, R.A. Vaishnav, A.G. Mustafa, Antioxidant therapies for traumatic brain injury, Neurotherapeutics 7 (2010) 51–61.
[55] W. Lo, T. Bravo, V. Jadhav, E. Titova, J.H. Zhang, J. Tang, NADPH oxidase inhibition improves neurological outcomes in surgically-induced brain injury, Neurosci. Lett. 414 (2007) 228–232.
[56] M.W. Ma, J. Wang, K.M. Dhandapani, R. Wang, D.W. Brann, NADPH oxidases in traumatic brain injury - promising therapeutic targets? Redox Biol. 16 (2018) 285–293.
[57] A.I. Casas, E. Geuss, P.W.M. Kleikers, S. Mencl, A.M. Herrmann, I. Buendia, et al., NOX4-dependent neuronal autotoxicity and BBB breakdown explain the superior sensitivity of the brain to ischemic damage, Proc. Natl. Acad. Sci. U. S. A. 114 (2017) 12315–12320.
[58] M.W. Ma, J. Wang, K.M. Dhandapani, D.W. Brann, Deletion of NADPH oxidase 4 reduces severity of traumatic brain injury, Free Radic. Biol. Med. 117 (2018) 66–75.
[59] B.P. Lucke-Wold, Z.J. Naser, A.F. Logsdon, R.C. Turner, K.E. Smith, M.J. Robson, et al., Amelioration of nicotinamide adenine dinucleotide phosphate-oxidase mediated stress reduces cell death after blast-induced traumatic brain injury, Transl. Res. 166 (2015) 509–528 (e1).
[60] S. Sciarretta, M. Volpe, J. Sadoshima, NOX4 regulates autophagy during energy deprivation, Autophagy 10 (2014) 699–701.
[61] D. Deliyanti, J.L. Wilkinson-Berka, Inhibition of NOX1/4 with GKT137831: a potential novel treatment to attenuate neuroglial cell inflammation in the retina, J. Neuroinflammation 12 (2015) 136.
[62] U.I. Onat, A.D. Yildirim, O. Tufanli, I. Cimen, B. Kocaturk, Z. Veli, et al., Intercepting the lipid-induced integrated stress response reduces atherosclerosis, J. Am. Coll. Cardiol. 73 (2019) 1149–1169.
[63] J. Duan, Q. Zhang, X. Hu, D. Lu, W. Yu, H. Bai, N(4)-acetylcytidine is required for sustained NLRP3 inflammasome activation via HMGB1 pathway in microglia, Cell. Signal. 58 (2019) 44–52.